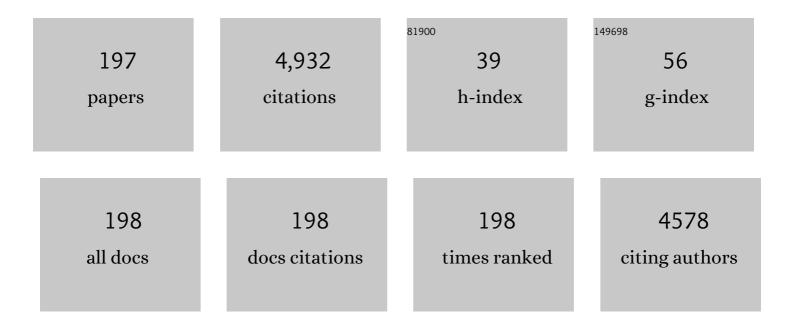
Ming-Yen Wey

List of Publications by Year in descending order

Source: https://exaly.com/author-pdf/8634022/publications.pdf Version: 2024-02-01



#	Article	IF	CITATIONS
1	Photo-induced poly(styrene-[C1mim][Tf2N])-supported hollow fiber ionic liquid membranes to enhance CO2 separation. Journal of CO2 Utilization, 2022, 56, 101871.	6.8	3
2	Excellent dispersion of solar light responsive photocatalyst in the different polymer films for easy recycling and sustainable hydrogen production. Solar Energy, 2022, 231, 949-957.	6.1	9
3	Carbon membrane for the application in gas separation: recent development and prospects. , 2022, , 177-214.		0
4	Effect of heat diffusivity for driving chain stitching of dual-type hybrid organosilica-derived membranes. Separation and Purification Technology, 2022, 290, 120848.	7.9	5
5	Development of physicochemically stable Z-scheme MIL-88A/g-C3N4 heterojunction photocatalyst with excellent charge transfer for improving acid red 1 dye decomposition efficiency. Applied Surface Science, 2022, 590, 152954.	6.1	12
6	Solvent effects on diffusion channel construction of organosilica membrane with excellent CO2 separation properties. Journal of Membrane Science, 2021, 618, 118758.	8.2	17
7	Positive effects of a halloysite-supported Cu/Co catalyst fabricated by a urea-driven deposition precipitation method on the CO-SCR reaction and SO ₂ poisoning. Catalysis Science and Technology, 2021, 11, 3456-3465.	4.1	9
8	Insights into the Role of Polymer Conformation on the Cutoff Size of Carbon Molecular Sieving Membranes for Hydrogen Separation and Its Novel Pore Size Detection Technology. ACS Applied Materials & Interfaces, 2021, 13, 5165-5175.	8.0	14
9	Impacts of Green Synthesis Process on Asymmetric Hybrid PDMS Membrane for Efficient CO2/N2 Separation. Membranes, 2021, 11, 59.	3.0	9
10	Highly abrasion and coking-resistance core-shell catalyst for hydrogen-rich syngas production from waste plastics in a two-staged fluidized bed reactor. Applied Catalysis A: General, 2021, 612, 117989.	4.3	9
11	Effect of polystyrene characteristic on photocatalytic hydrogen production by porous polystyrene photocatalyst film under simulated solar light irradiation. International Journal of Hydrogen Energy, 2021, 46, 11597-11606.	7.1	5
12	Fabrication of waterproof gas separation membrane from plastic waste for CO2 separation. Environmental Research, 2021, 195, 110760.	7.5	10
13	High loading and high-selectivity H2 purification using SBC@ZIF based thin film composite hollow fiber membranes. Journal of Membrane Science, 2021, 626, 119191.	8.2	10
14	In situ phase transformation of polytypic zinc-blende/wurtzite copper indium sulfide via a facile polyol method to boost visible-light photocatalytic performance. Chemosphere, 2021, 277, 130348.	8.2	6
15	Synthesis of Ni@Al2O3 nanocomposite with superior activity and stability for hydrogen production from plastic-derived syngas by CO2-sorption-enhanced reforming. International Journal of Hydrogen Energy, 2021, 46, 39728-39735.	7.1	7
16	Dual immobilization of Pd Cu nanoparticles on halloysite nanotubes by CTAB and PVP for automobile exhaust elimination. Applied Clay Science, 2021, 214, 106299.	5.2	7
17	Highly Permeable Mixed Matrix Hollow Fiber Membrane as a Latent Route for Hydrogen Purification from Hydrocarbons/Carbon Dioxide. Membranes, 2021, 11, 865.	3.0	4
18	Thin carbon hollow fiber membrane with Knudsen diffusion for hydrogen/alkane separation: Effects of hollow fiber module design and gas flow mode. International Journal of Hydrogen Energy, 2020, 45, 7290-7302.	7.1	15

Ming-Yen Wey

#	Article	IF	CITATIONS
19	Sintering-resistant, highly thermally stable and well-dispersed Pd@CeO2/halloysite as an advanced three-way catalyst. Science of the Total Environment, 2020, 707, 136137.	8.0	13
20	Recycling waste plastics as hollow fiber substrates to improve the anti-wettability of supported ionic liquid membranes for CO2 separation. Journal of Cleaner Production, 2020, 276, 124194.	9.3	11
21	The Viable Fabrication of Gas Separation Membrane Used by Reclaimed Rubber from Waste Tires. Polymers, 2020, 12, 2540.	4.5	8
22	Design of catalysts comprising a nickel core and ceria shell for hydrogen production from plastic waste gasification: an integrated test for anti-coking and catalytic performance. Catalysis Science and Technology, 2020, 10, 3975-3984.	4.1	17
23	Co-production of carbon nanotubes and hydrogen from waste plastic gasification in a two-stage fluidized catalytic bed. Renewable Energy, 2020, 159, 10-22.	8.9	57
24	Design of a thermally resistant core@shell/halloysite catalyst with optimized structure and surface properties for a Pd-only three-way catalyst. Applied Catalysis A: General, 2020, 602, 117732.	4.3	15
25	Synthesis of carbon nanotubes with controllable diameter by chemical vapor deposition of methane using Fe@Al2O3 core–shell nanocomposites. Chemical Engineering Science, 2020, 217, 115541.	3.8	17
26	Uniformity control and ultraâ€micropore development of tubular carbon membrane for light gas separation. AICHE Journal, 2020, 66, e16226.	3.6	6
27	Facile approach for Z-scheme type Pt/g-C3N4/SrTiO3 heterojunction semiconductor synthesis via low-temperature process for simultaneous dyes degradation and hydrogen production. International Journal of Hydrogen Energy, 2020, 45, 13330-13339.	7.1	25
28	PVA/Pt/N-TiO2/SrTiO3 porous films with adjustable pore size for hydrogen production under simulated sunlight. Journal of Colloid and Interface Science, 2020, 573, 158-164.	9.4	7
29	Synthesis of solar-light responsive Pt/g-C3N4/SrTiO3 composite for improved hydrogen production: Investigation of Pt/g-C3N4/SrTiO3 synthetic sequences. International Journal of Hydrogen Energy, 2019, 44, 21413-21423.	7.1	29
30	Reuse of reclaimed tire rubber for gas-separation membranes prepared by hot-pressing. Journal of Cleaner Production, 2019, 237, 117739.	9.3	24
31	Thermal degradation of waste plastics in a two-stage pyrolysis-catalysis reactor over core-shell type catalyst. Journal of Analytical and Applied Pyrolysis, 2019, 142, 104641.	5.5	31
32	Tuning thermal expansion behavior and surface roughness of tubular Al2O3 substrates for fabricating high-performance carbon molecular sieving membranes for H2 separation. International Journal of Hydrogen Energy, 2019, 44, 24746-24758.	7.1	8
33	Acceleration of acid red 1 dye decolorization efficiency by adding methanol with simultaneous hydrogen production. International Journal of Environmental Science and Technology, 2019, 16, 8355-8362.	3.5	3
34	Hydrogen promotion by Co/SiO2@HZSM-5 core-shell catalyst for syngas from plastic waste gasification: The combination of functional materials. International Journal of Hydrogen Energy, 2019, 44, 13480-13489.	7.1	20
35	Core-shell design and well-dispersed Pd particles for three-way catalysis: Effect of halloysite nanotubes functionalized with Schiff base. Science of the Total Environment, 2019, 675, 397-407.	8.0	15
36	Interfacial interaction between CMS layer and substrate: Critical factors affecting membrane microstructure and H2 and CO2 separation performance from CH4. Journal of Membrane Science, 2019, 580, 49-61.	8.2	20

#	Article	IF	CITATIONS
37	Effect of Preparation Solvent and Calcination Atmosphere on Ni@SiO 2 Catalyst for Simultaneous Production of Hydrogen and Carbon Nanotubes from Simulated Plastic Waste Syngas. Energy Technology, 2019, 7, 1800586.	3.8	8
38	Creation of tiny defects in ZIF-8 by thermal annealing to improve the CO2/N2 separation of mixed matrix membranes. Journal of Membrane Science, 2019, 572, 410-418.	8.2	30
39	Effects of Temperature and Equivalence Ratio on Carbon Nanotubes and Hydrogen Production from Waste Plastic Gasification in Fluidized Bed. Energy & Fuels, 2018, 32, 5462-5470.	5.1	42
40	Reuse of bottom ash and fly ash from mechanical-bed and fluidized-bed municipal incinerators in manufacturing lightweight aggregates. Ceramics International, 2018, 44, 12691-12696.	4.8	44
41	Facile synthesis of CO2-selective membrane derived from butyl reclaimed rubber (BRR) for efficient CO2 separation. Journal of CO2 Utilization, 2018, 25, 226-234.	6.8	15
42	Enhancing the CO2 plasticization resistance of PS mixed-matrix membrane by blunt zeolitic imidazolate framework. Journal of CO2 Utilization, 2018, 25, 79-88.	6.8	16
43	Enrichment of Hydrogen Production from Biomassâ€Gasificationâ€Derived Syngas over Spinelâ€Type Aluminateâ€Supported Nickel Catalysts. Energy Technology, 2018, 6, 318-325.	3.8	9
44	Excellent dispersion and charge separation of SrTiO3-TiO2 nanotube derived from a two-step hydrothermal process for facilitating hydrogen evolution under sunlight irradiation. Solar Energy, 2018, 159, 751-759.	6.1	11
45	Catalytic Methane Decomposition to Hydrogen over a Surfaceâ€Protected Coreâ€Shell Ni@SiO ₂ Catalyst. Chemical Engineering and Technology, 2018, 41, 1448-1456.	1.5	11
46	Photocatalytic conversion of ethylenediaminetetraacetic acid dissolved in real electroplating wastewater to hydrogen in a solar light-responsive system. Water Science and Technology, 2018, 77, 2851-2857.	2.5	4
47	Green Route for Hydrogen Evolution from Real Electroplating Waste Liquids Induced by a Solar Light Responsive Photocatalyst. ACS Sustainable Chemistry and Engineering, 2017, 5, 2146-2153.	6.7	7
48	Effect of copolymer microphase-separated structures on the gas separation performance and aging properties of SBC-derived membranes. Journal of Membrane Science, 2017, 529, 63-71.	8.2	10
49	Design of a solar light-responsive metal oxide/CdS/SrTiO 3 catalyst with enhanced charge separation for hydrogen evolution. Solar Energy, 2017, 147, 240-247.	6.1	23
50	Ni/SiO 2 core–shell catalysts for catalytic hydrogen production from waste plastics-derived syngas. International Journal of Hydrogen Energy, 2017, 42, 11239-11251.	7.1	31
51	Structure-controlled mesoporous SBA-15-derived mixed matrix membranes for H2 purification and CO2 capture. International Journal of Hydrogen Energy, 2017, 42, 11379-11391.	7.1	21
52	Feasibility of using waste polystyrene as a membrane material for gas separation. Chemical Engineering Research and Design, 2016, 111, 204-217.	5.6	30
53	Enhanced optical and electronic properties of a solar light-responsive photocatalyst for efficient hydrogen evolution by SrTiO3/TiO2 nanotube combination. Solar Energy, 2016, 134, 52-63.	6.1	35
54	Carbon nanotube and hydrogen production from waste plastic gasification over Ni/Al–SBA-15 catalysts: effect of aluminum content. RSC Advances, 2016, 6, 40731-40740.	3.6	27

#	Article	IF	CITATIONS
55	A novel technique using reclaimed tire rubber for gas separation membranes. Journal of Membrane Science, 2016, 520, 314-325.	8.2	24
56	Sustainable hydrogen production from electroplating wastewater over a solar light responsive photocatalyst. RSC Advances, 2016, 6, 71273-71281.	3.6	10
57	Effect of co-contaminated soil mixtures as fixed/fluidized bed media on pollutants emission under thermal treatment. International Journal of Environmental Science and Technology, 2016, 13, 519-528.	3.5	9
58	Thermal treatment of soil co-contaminated with lube oil and heavy metals in a low-temperature two-stage fluidized bed incinerator. Applied Thermal Engineering, 2016, 93, 131-138.	6.0	29
59	The different properties of lightweight aggregates with the fly ashes of fluidized-bed and mechanical incinerators. Construction and Building Materials, 2015, 101, 380-388.	7.2	20
60	Characterization and photoactivity of Pt/N-doped TiO2 synthesized through a sol–gel process at room temperature. Journal of Nanoparticle Research, 2015, 17, 1.	1.9	6
61	Influence of thermal treatment atmosphere on photogenerated charge separation of Pt/N–TiO2/SrTiO3 for efficient hydrogen evolution. Journal of Materials Science, 2015, 50, 5873-5885.	3.7	9
62	Determination of the Pb, Cr, and Cd distribution patterns with various chlorine additives in the bottom ashes of a low-temperature two-stage fluidized bed incinerator by chemical sequential extraction. Journal of Hazardous Materials, 2015, 295, 86-96.	12.4	5
63	Determination of Emission Characteristics during Thermal Treatment of Lube Oil and Heavy Metal Co-Contaminated Soil by Fluidized Bed Combustion. Journal of Environmental Engineering, ASCE, 2015, 141, .	1.4	5
64	The influence of matrix structure and thermal annealing-hydrophobic layer on the performance and durability of carbon molecular sieving membrane during physical aging. Journal of Membrane Science, 2015, 495, 294-304.	8.2	12
65	The density and crystallinity properties of PPO-silica mixed-matrix membranes produced via the in situ sol-gel method for H2/CO2 separation. II: Effect of thermal annealing treatment. Chemical Engineering Research and Design, 2015, 104, 319-332.	5.6	33
66	Cadmium Stabilization Efficiency and Leachability by CdAl ₄ O ₇ Monoclinic Structure. Environmental Science & amp; Technology, 2015, 49, 14452-14459.	10.0	37
67	Effects of Nickel Species on Ni/Al ₂ O ₃ Catalysts in Carbon Nanotube and Hydrogen Production by Waste Plastic Gasification: Bench- and Pilot-Scale Tests. Energy & Fuels, 2015, 29, 8178-8187.	5.1	73
68	Photocatalytic conversion of simulated EDTA wastewater to hydrogen by pH-resistant Pt/TiO2–activated carbon photocatalysts. Renewable Energy, 2015, 75, 266-271.	8.9	48
69	Study of the low-temperature two-stage fluidized bed incineration: Influence of the second-stage sand bed operating conditions on pollutant emission. Applied Thermal Engineering, 2015, 75, 592-599.	6.0	9
70	Hydrogen production through methanol steam reforming: Effect of synthesis parameters on Ni–Cu/CaO–SiO 2 catalysts activity. International Journal of Hydrogen Energy, 2014, 39, 19494-19501.	7.1	44
71	Effects of membrane compositions and operating conditions on the filtration and backwashing performance of the activated carbon polymer composite membranes. Desalination, 2014, 352, 181-189.	8.2	12
72	A carbon gutter layer-modified α-Al2O3 substrate for PPO membrane fabrication and CO2 separation. Journal of Membrane Science, 2014, 454, 51-61.	8.2	12

#	Article	IF	CITATIONS
73	Characterization of N-doped TiO2 nanoparticles supported on SrTiO3 via a sol–gel process. Journal of Nanoparticle Research, 2014, 16, 1.	1.9	8
74	Gaseous organic emissions during air gasification of woody waste: effect of bed agglomeration/defluidization. Fuel Processing Technology, 2014, 128, 104-110.	7.2	11
75	Preparation of PPO-silica mixed matrix membranes by in-situ sol–gel method for H2/CO2 separation. International Journal of Hydrogen Energy, 2014, 39, 17178-17190.	7.1	41
76	Improving the mechanical strength and gas separation performance of CMS membranes by simply sintering treatment of α-Al2O3 support. Journal of Membrane Science, 2014, 453, 603-613.	8.2	32
77	Development of a low-temperature two-stage fluidized bed incinerator for controlling heavy-metal emission in flue gases. Applied Thermal Engineering, 2014, 62, 706-713.	6.0	13
78	Removal of NO and fly ash over a carbon supported catalyst: Effects of fly ash concentration and operating time. Powder Technology, 2013, 239, 239-247.	4.2	7
79	Effect of MFI zeolite intermediate layers on gas separation performance of carbon molecular sieve (CMS) membranes. Journal of Membrane Science, 2013, 446, 220-229.	8.2	26
80	CuO/CeO2 catalysts prepared with different cerium supports for CO oxidation at low temperature. Materials Chemistry and Physics, 2013, 141, 512-518.	4.0	18
81	Development of CMS/Al2O3-supported PPO composite membrane for hydrogen separation. International Journal of Hydrogen Energy, 2013, 38, 3092-3104.	7.1	12
82	Woody waste air gasification in fluidized bed with Ca- and Mg-modified bed materials and additives. Applied Thermal Engineering, 2013, 53, 42-48.	6.0	12
83	The properties and filtration efficiency of activated carbon polymer composite membranes for the removal of humic acid. Desalination, 2013, 313, 166-175.	8.2	73
84	Design of a Pt/TiO2–xNx/SrTiO3 triplejunction for effective photocatalytic H2 production under solar light irradiation. Chemical Engineering Journal, 2013, 223, 854-859.	12.7	24
85	Copper catalysts prepared via microwave-heated polyol process for preferential oxidation of CO in H2-rich streams. International Journal of Hydrogen Energy, 2013, 38, 100-108.	7.1	12
86	Evaluating the Relationships between Pb Species and Leaching Properties in Simulated MSWI Fly Ash with Thermal Treatment by ESCA. Journal of Environmental Engineering, ASCE, 2012, 138, 632-636.	1.4	2
87	Copper emission during thermal treatment of simulated copper sludge. Environmental Technology (United Kingdom), 2012, 33, 17-25.	2.2	3
88	The influences of microwave irradiation and polyol precursor pH on Cu/AC catalyst and its CO oxidation performance. Journal of Nanoparticle Research, 2012, 14, 1.	1.9	3
89	Effect of agglomeration/defluidization on hydrogen generation during fluidized bed air gasification of modified biomass. International Journal of Hydrogen Energy, 2012, 37, 1409-1417.	7.1	15
90	Hydrogen production by biomass gasification in a fluidized-bed reactor promoted by an Fe/CaO catalyst. International Journal of Hydrogen Energy, 2012, 37, 6511-6518.	7.1	113

#	Article	IF	CITATIONS
91	Catalytic upgrading of syngas from fluidized bed air gasification of sawdust. Bioresource Technology, 2012, 110, 670-675.	9.6	34
92	Influence of support structure on the permeation behavior of polyetherimide-derived carbon molecular sieve composite membrane. Journal of Membrane Science, 2012, 405-406, 250-260.	8.2	46
93	Simulation of agglomeration/defluidization inhibition process in aluminum–sodium system by experimental and thermodynamic approaches. Powder Technology, 2012, 224, 395-403.	4.2	9
94	Emission of carbon dioxide in municipal solid waste incineration in Taiwan: A comparison with thermal power plants. International Journal of Greenhouse Gas Control, 2011, 5, 889-898.	4.6	28
95	Effect of alkali concentrations and operating conditions on agglomeration/defluidization behavior during fluidized bed air gasification. Powder Technology, 2011, 214, 443-446.	4.2	18
96	Properties and H2 production ability of Pt photodeposited on the anatase phase transition of nitrogen-doped titanium dioxide. International Journal of Hydrogen Energy, 2011, 36, 9479-9486.	7.1	32
97	Removals of fly ash and NO in a fluidized-bed reactor with CuO/activated carbon catalysts. Journal of Hazardous Materials, 2011, 187, 190-198.	12.4	13
98	Effect of SBA-15 texture on the gas separation characteristics of SBA-15/polymer multilayer mixed matrix membrane. Journal of Membrane Science, 2011, 369, 550-559.	8.2	42
99	Catalytic removal of NO and PAHs over AC-supported catalysts from incineration flue gas: Bench-scale and pilot-plant tests. Chemical Engineering Journal, 2011, 169, 135-143.	12.7	21
100	Effect of particle agglomeration on heavy metals adsorption by Al- and Ca-based sorbents during fluidized bed incineration. Fuel Processing Technology, 2011, 92, 2089-2098.	7.2	58
101	Effects of microwave power and polyvinyl pyrrolidone on microwave polyol process of carbon-supported Cu catalysts for CO oxidation. Materials Science and Engineering B: Solid-State Materials for Advanced Technology, 2011, 176, 745-749.	3.5	8
102	NO removal by activated carbon-supported copper catalysts prepared by impregnation, polyol, and microwave heated polyol processes. Applied Catalysis A: General, 2011, 397, 234-240.	4.3	42
103	Fabrication and characterization of PPO/PVP blend carbon molecular sieve membranes for H2/N2 and H2/CH4 separation. Journal of Membrane Science, 2011, 372, 387-395.	8.2	80
104	Effects of crosslinking modification on the O ₂ /N ₂ separation characteristics of poly(phenyl sulfone)/poly(bisphenol Aâ€ <i>co</i> â€4â€nitrophthalic) Tj ETQq0 0 0 rgBT /Overlock 10 Tf 50 22 116, 1254-1263.	22 Td (anh 2.6	nydŗideâ€∢i>c
105	An efficient composite growing N-doped TiO2 on multi-walled carbon nanotubes through sol–gel process. Journal of Nanoparticle Research, 2010, 12, 2503-2510.	1.9	23
106	Study of SBA-15 supported catalysts for toluene and NO removal: the effect of promoters (Co, Ni, Mn,) Tj ETQq0	0 0 rgBT / 1.7gBT /	Overlock 10
107	Effect of Cu species on leaching behavior of simulated copper sludge after thermal treatment: ESCA analysis. Journal of Hazardous Materials, 2010, 179, 1106-1110.	12.4	3
108	Evaluation of SO2 oxidation and fly ash filtration by an activated carbon fluidized-bed reactor: The	6.4	21

108 effects of acid modification, copper addition and operating condition. Fuel, 2010, 89, 732-742.

#	Article	IF	CITATIONS
109	Activity and characterization of Rh/Al2O3 and Rh–Na/Al2O3 catalysts for the SCR of NO with CO in the presence of SO2 and HCl. Fuel, 2010, 89, 1919-1927.	6.4	18
110	Effect of dry/wet-phase inversion method on fabricating polyetherimide-derived CMS membrane for H2/N2 separation. International Journal of Hydrogen Energy, 2010, 35, 1650-1658.	7.1	44
111	Fabrication and characterization of poly(phenylene oxide)/SBA-15/carbon molecule sieve multilayer mixed matrix membrane for gas separation. International Journal of Hydrogen Energy, 2010, 35, 6971-6983.	7.1	57
112	Photocatalytic properties of redox-treated Pt/TiO2 photocatalysts for H2 production from an aqueous methanol solution. International Journal of Hydrogen Energy, 2010, 35, 7699-7705.	7.1	78
113	Catalytic activity of copper-supported catalyst for NO reduction in the presence of oxygen: Fitting of calcination temperature and copper loading. Materials Science and Engineering B: Solid-State Materials for Advanced Technology, 2010, 175, 100-107.	3.5	13
114	Mechanisms of particle agglomeration and inhibition approach in the existence of heavy metals during fluidized bed incineration. Chemical Engineering Science, 2010, 65, 4955-4966.	3.8	14
115	Estimating the feasibility of raw carbon nanotubes used as catalyst for CO oxidation. , 2010, , .		0
116	Enhanced O <inf>2</inf> /N <inf>2</inf> separation performance of poly(phenylene) Tj ETQ 2010, , .	<u>)</u> q0 0 0 rgB	T /Overlock I 2
117	An effective method for controlling the nanoparticle size of anatase TiO <inf>2</inf> . , 2010, , .		0
118	Filtration of nanoparticles by a fluidized-bed adsorption reactor during toluene adsorption. , 2010, , .		0
119	Removal the Coal Ash, NO, and SO ₂ Simultaneously by the Fluidized-Bed Catalyst Reactor. Energy & Fuels, 2010, 24, 1711-1719.	5.1	6
120	Study on Pb and PAHs Emission Levels of Heavy Metals- and PAHs-Contaminated Soil during Thermal Treatment Process. Journal of Environmental Engineering, ASCE, 2010, 136, 112-118.	1.4	14
121	Effect of operating conditions on emission concentration of PAHs during fluidized bed air gasification of biomass. , 2010, , .		2
122	The comparison between the polyol process and the impregnation method for the preparation of CNT-supported nanoscale Cu catalyst. Chemical Engineering Journal, 2009, 145, 461-467.	12.7	25
123	Evaluating the potential of CNT-supported Co catalyst used for gas pollution removal in the incineration flue gas. Journal of Environmental Management, 2009, 90, 1884-1892.	7.8	15
124	Effects of the ratio of Cu/Co and metal precursors on the catalytic activity over Cu-Co/Al2O3 prepared using the polyol process. Materials Science and Engineering B: Solid-State Materials for Advanced Technology, 2009, 157, 105-112.	3.5	14
125	Improving the Activity of Rh/Al2O3 Catalyst for NO Reduction by Na Addition in the Presences of H2O and O2. Catalysis Letters, 2009, 130, 517-524.	2.6	2
126	Al2O3-supported Cu–Co bimetallic catalysts prepared with polyol process for removal of BTEX and PAH in the incineration flue gas. Fuel, 2009, 88, 340-347.	6.4	32

#	Article	IF	CITATIONS
127	The activity of Rh/Al2O3 and Rh–Na/Al2O3 catalysts for PAHs removal in the waste incineration processes: Effects of particulates, heavy metals, and acid gases. Fuel, 2009, 88, 1563-1571.	6.4	7
128	Catalytic removal of NO in waste incineration processes over Rh/Al2O3 and Rh–Na/Al2O3: Effects of particulates, heavy metals, SO2 and HCl. Fuel Processing Technology, 2009, 90, 576-582.	7.2	12
129	Preparation and characterization of multi-walled carbon nanotube/PBNPI nanocomposite membrane for H2/CH4 separation. International Journal of Hydrogen Energy, 2009, 34, 8707-8715.	7.1	104
130	Evaluation of the distribution patterns of Pb, Cu and Cd from MSWI fly ash during thermal treatment by sequential extraction procedure. Journal of Hazardous Materials, 2009, 162, 1000-1006.	12.4	78
131	Effects of particulates, heavy metals and acid gas on the removals of NO and PAHs by V2O5–WO3 catalysts in waste incineration system. Journal of Hazardous Materials, 2009, 170, 239-246.	12.4	11
132	Collection of SiO2, Al2O3 and Fe2O3 particles using a gas-solid fluidized bed filter. Journal of Hazardous Materials, 2009, 171, 102-110.	12.4	17
133	Inhibition and promotion: The effect of earth alkali metals and operating temperature on particle agglomeration/defluidization during incineration in fluidized bed. Powder Technology, 2009, 189, 57-63.	4.2	51
134	Catalytic treating of gas pollutants over cobalt catalyst supported on porous carbons derived from rice husk and carbon nanotube. Applied Catalysis B: Environmental, 2009, 90, 652-661.	20.2	21
135	Preparation and characterization of carbon molecular sieve membranes for gas separation—the effect of incorporated multi-wall carbon nanotubes. Desalination, 2009, 240, 40-45.	8.2	58
136	Study of the activity and backscattered electron image of Pt/CNTs prepared by the polyol process for flue gas purification. Applied Catalysis A: General, 2009, 354, 57-62.	4.3	12
137	Effects of oxygen and hydrogen chloride on NO removal efficiency by Rh/Al2O3 and Rh–Na/Al2O3 catalysts. Applied Catalysis A: General, 2009, 359, 88-95.	4.3	7
138	Effects of Agglomeration Processes on the Emission Characteristics of Heavy Metals under Different Waste Compositions and the Addition of Al and Ca Inhibitors in Fluidized Bed Incineration. Energy & Fuels, 2009, 23, 4325-4336.	5.1	8
139	Effects of H2O and Particles on the Simultaneous Removal of SO2 and Fly Ash Using a Fluidized-Bed Sorbent/Catalyst Reactor. Industrial & Engineering Chemistry Research, 2009, 48, 10541-10550.	3.7	3
140	Comparison of visible-light-driven routes of anion-doped TiO2 and composite photocatalyst. Journal of the Ceramic Society of Japan, 2009, 117, 753-758.	1.1	22
141	The prospect and development of incinerators for municipal solid waste treatment and characteristics of their pollutants in Taiwan. Applied Thermal Engineering, 2008, 28, 2305-2314.	6.0	41
142	Effects of Na, Cu, Ni and Co Modifications on the Activity and Characteristics of Rh/Al2O3 Catalysts for NO Reduction. Catalysis Letters, 2008, 126, 207-211.	2.6	5
143	Emission of Pb and PAHs from thermally co-treated MSWI fly ash and bottom ash process. Journal of Hazardous Materials, 2008, 150, 27-36.	12.4	23
144	Characterizing PAH emission concentrations in ambient air during a large-scale joss paper open-burning event. Journal of Hazardous Materials, 2008, 156, 223-229.	12.4	16

#	Article	IF	CITATIONS
145	Effects of sodium modification, different reductants and SO2 on NO reduction by Rh/Al2O3 catalysts at excess O2 conditions. Journal of Hazardous Materials, 2008, 156, 348-355.	12.4	20
146	The size, shape, and dispersion of active sites on AC-supported copper nanocatalysts with polyol process: The effect of precursors. Applied Catalysis A: General, 2008, 344, 36-44.	4.3	36
147	The effect of aluminum inhibition on the defluidization behavior and generation of pollutants in fluidized bed incineration. Fuel Processing Technology, 2008, 89, 1227-1236.	7.2	20
148	Preparation and characterization of PPSU/PBNPI blend membrane for hydrogen separation. International Journal of Hydrogen Energy, 2008, 33, 4178-4182.	7.1	34
149	A comparison of carbon/nanotube molecular sieve membranes with polymer blend carbon molecular sieve membranes for the gas permeation application. Microporous and Mesoporous Materials, 2008, 113, 499-510.	4.4	83
150	Partitioning and Emission Characteristics of Pb and Organics during Fluidized Bed Thermal Treatment of Municipal Solid Waste Incineration (MSWI) Fly Ash. Energy & amp; Fuels, 2008, 22, 3789-3797.	5.1	8
151	EMISSION CHARACTERISTICS OF CHLOROBENZENES, CHLOROPHENOLS AND DIOXINS DURING WASTE INCINERATION WITH DIFFERENT ADDITIVES. Combustion Science and Technology, 2007, 179, 1039-1058.	2.3	7
152	Application of polyol process to prepare AC-supported nanocatalyst for VOC oxidation. Applied Catalysis A: General, 2007, 325, 163-174.	4.3	54
153	Filtration of fly ash using fluidized bed at 300–500°C. Fuel, 2007, 86, 161-168.	6.4	14
154	The performance of CNT as catalyst support on CO oxidation at low temperature. Fuel, 2007, 86, 1153-1161.	6.4	51
155	Simultaneous removal of VOC and NO by activated carbon impregnated with transition metal catalysts in combustion flue gas. Fuel Processing Technology, 2007, 88, 557-567.	7.2	97
156	Filtration of nano-particles by a gas–solid fluidized bed. Journal of Hazardous Materials, 2007, 147, 618-624.	12.4	20
157	Effects of acid treatments of activated carbon on its physiochemical structure as a support for copper oxide in DeSO2 reaction catalysts. Chemosphere, 2006, 62, 756-766.	8.2	63
158	Effects of metal precursor in the sol–gel synthesis on the physicochemical properties of Pd/Al2O3–CeO2 catalyst: CO oxidation. Journal of Non-Crystalline Solids, 2006, 352, 2166-2172.	3.1	4
159	Formations and controls of HCl and PAHs by different additives during waste incineration. Fuel, 2006, 85, 755-763.	6.4	48
160	Prediction of defluidization time of alkali composition at various operating conditions during incineration. Powder Technology, 2006, 161, 150-157.	4.2	17
161	Thermal treatment of the fly ash from municipal solid waste incinerator with rotary kiln. Journal of Hazardous Materials, 2006, 137, 981-989.	12.4	86
162	Comparison of the characteristics of bottom and fly ashes generated from various incineration processes. Journal of Hazardous Materials, 2006, 138, 594-603.	12.4	138

#	Article	IF	CITATIONS
163	The effect of ash and filter media characteristics on particle filtration efficiency in fluidized bed. Journal of Hazardous Materials, 2005, 121, 175-181.	12.4	29
164	Emission characteristics of organic and heavy metal pollutants in fluidized bed incineration during the agglomeration/defluidization process. Combustion and Flame, 2005, 143, 139-149.	5.2	27
165	Influence of hydrodynamic parameters on particle attrition during fluidization at high temperature. Korean Journal of Chemical Engineering, 2005, 22, 154-160.	2.7	31
166	Filtration of Fly Ash Using a Fluidized-Bed Filter. Journal of the Air and Waste Management Association, 2005, 55, 181-193.	1.9	14
167	Dynamic purification of coal ash by a gas–solid fluidized bed. Chemosphere, 2005, 60, 1341-1348.	8.2	12
168	Simultaneous treatment of organic compounds, CO, and NOx in the incineration flue gas by three-way catalyst. Applied Catalysis B: Environmental, 2004, 48, 25-35.	20.2	37
169	Effect of concentration of bed materials on combustion efficiency during incineration. Energy, 2004, 29, 125-136.	8.8	8
170	The effect of mineral compositions of waste and operating conditions on particle agglomeration/defluidization during incineration. Fuel, 2004, 83, 2335-2343.	6.4	68
171	Study of SO2 adsorption and thermal regeneration over activated carbon-supported copper oxide catalysts. Carbon, 2004, 42, 2269-2278.	10.3	111
172	Relationship between pressure fluctuations and generation of organic pollutants with different particle size distributions in a fluidized bed incinerator. Chemosphere, 2004, 56, 911-922.	8.2	10
173	Effects of high temperature and combustion on fluidized material attrition in a fluidized bed. Korean Journal of Chemical Engineering, 2003, 20, 1123-1130.	2.7	24
174	Carbon materials as catalyst supports for SO2 oxidation: catalytic activity of CuO–AC. Carbon, 2003, 41, 139-149.	10.3	93
175	Catalytic removal of SO2, NO and HCl from incineration flue gas over activated carbon-supported metal oxides. Carbon, 2003, 41, 1079-1085.	10.3	98
176	Control of acid gases using a fluidized bed adsorber. Journal of Hazardous Materials, 2003, 101, 259-272.	12.4	32
177	Thermal Treatment for Incinerator Ash: Evaporation and Leaching Rates of Metals. Journal of Environmental Engineering, ASCE, 2003, 129, 258-266.	1.4	8
178	Oxidation of organic pollutants in incineration flue gas by a fluidized palladium catalyst. Combustion Science and Technology, 2003, 175, 1211-1236.	2.3	6
179	The Competitive Adsorption of Heavy Metals under Various Incineration Conditions Journal of Chemical Engineering of Japan, 2003, 36, 243-249.	0.6	2
180	The Utilization of Catalyst Sorbent in Scrubbing Acid Gases from Incineration Flue Gas. Journal of the Air and Waste Management Association, 2002, 52, 449-458.	1.9	10

#	Article	IF	CITATIONS
181	Catalytic Oxidation of Organic Compounds in Incineration Flue Gas by a Commercial Palladium Catalyst. Journal of the Air and Waste Management Association, 2002, 52, 198-207.	1.9	7
182	The effect of particle size distribution on minimum fluidization velocity at high temperature. Powder Technology, 2002, 126, 297-301.	4.2	124
183	The Capture of Heavy Metals from Incineration Using a Spray Dryer Integrated with a Fabric Filter Using Various Additives. Journal of the Air and Waste Management Association, 2001, 51, 983-991.	1.9	5
184	Adsorption Mechanism of Heavy Metals on Sorbents during Incineration. Journal of Environmental Engineering, ASCE, 2001, 127, 63-69.	1.4	47
185	The influence of heavy metals on partitioning of PAHs during incineration. Journal of Hazardous Materials, 2000, 77, 77-87.	12.4	32
186	Control of Incinerator Organics by Fluidized Bed Activated Carbon Adsorber. Journal of Environmental Engineering, ASCE, 2000, 126, 985-992.	1.4	23
187	Influence of Operating Conditions on the Formation of Heavy Metal Compounds During Incineration. Journal of the Air and Waste Management Association, 1999, 49, 444-453.	1.9	10
188	The Effects of Chloride Additives on Adsorption of Heavy Metals during Incineration. Journal of the Air and Waste Management Association, 1999, 49, 1116-1120.	1.9	6
189	Stability of heavy metals in bottom ash and fly ash under various incinerating conditions. Journal of Hazardous Materials, 1998, 57, 145-154.	12.4	24
190	The influence of heavy metals on the formation of organics and HCl during incinerating of PVC-containing waste. Journal of Hazardous Materials, 1998, 60, 259-270.	12.4	40
191	Two-stage simulation of the major heavy-metal species under various incineration conditions. Environment International, 1998, 24, 451-466.	10.0	39
192	The Relationship between the Quantity of Heavy Metal and PAHs in Fly Ash. Journal of the Air and Waste Management Association, 1998, 48, 750-756.	1.9	24
193	The Major Species of Heavy Metal Aerosol Resulting from Water Cooling Systems and Spray Dryer Systems during Incineration Processes. Journal of the Air and Waste Management Association, 1998, 48, 1069-1076.	1.9	5
194	Mass and Elemental Size Distribution of Chromium, Lead and Cadmium under Various Incineration Conditions Journal of Chemical Engineering of Japan, 1998, 31, 506-517.	0.6	14
195	Theoretical and Experimental Study of Metal Capture during Incineration Process. Journal of Environmental Engineering, ASCE, 1997, 123, 1100-1106.	1.4	41
196	The behavior of heavy metal Cr,Pb and Cd during waste incineration in fluidized bed under various chlorine additives Journal of Chemical Engineering of Japan, 1996, 29, 494-500.	0.6	42
197	The Autothermal Pyrolysis of Waste Tires. Journal of the Air and Waste Management Association, 1995, 45, 855-863.	1.9	31